Inorganica Chimica Acta 498 (2019) 119136

Contents lists available at ScienceDirect

Inorganica Chimica Acta

journal homepage: www.elsevier.com/locate/ica

Research paper

Facile synthesis of a luminescent copper(I) coordination polymer containing a flexible benzotriazole-based ligand: An effective catalyst for three-component azide-alkyne cycloaddition

Nelson Nuñez-Dallos[a,b], Alvaro Muñoz-Castro[c], Mauricio Fuentealba[d], Edwin G. Pérez[e,*], John J. Hurtado[a,*]

[a] Departamento de Química, Universidad de los Andes, Carrera 1 No. 18A-12, 111711 Bogotá, Colombia
[b] Departamento de Química y Bioquímica, Facultad de Ciencias e Ingeniería, Universidad de Boyacá, Carrera 2ª Este No. 64-169, 150003 Tunja, Colombia
[c] Laboratorio de Química Inorgánica y Materiales Moleculares, Universidad Autónoma de Chile, Llano Subercaceaux 2801, San Miguel, Santiago, Chile
[d] Instituto de Química, Pontificia Universidad Católica de Valparaíso, Casilla 4059 Valparaíso, Chile
[e] Departamento de Química Orgánica, Facultad de Química y de Farmacia, Pontificia Universidad Católica de Chile, Av. Vicuña Mackenna 4860, Santiago 7820436, Chile

ARTICLE INFO

Keywords:
Copper(I) coordination polymer
Luminescence
Catalysis
Azide-alkyne cycloaddition
Click chemistry

ABSTRACT

A straightforward method for the synthesis of a new luminescent copper(I) coordination polymer (CP) containing the ligand 1,3-bis(1*H*-benzotriazol-1-ylmethyl)benzene (L) through a self-assembly process with copper (I) iodide is reported. The CP was characterized by infrared, NMR, UV–Vis and photoluminescence spectroscopy, high resolution mass spectrometry (ESI), elemental and thermogravimetric analyses, single-crystal and powder X-ray diffraction, and relativistic density functional theory calculations. Furthermore, this one-dimensional copper(I) benzotriazole-based coordination polymer catalyzed the three-component azide-alkyne cycloaddition reaction to obtain 1,4-disubstituted 1,2,3-triazoles in good to excellent yields (up to 95%) from organic halides, sodium azide and terminal alkynes.

1. Introduction

Coordination polymers (CPs) based on d^{10} metal ions have been investigated recently because of their potential applications in sensing [1], luminescent materials [2,3] and catalysis [4–6]. Among CPs, copper(I) CPs are attractive as catalysts for various organic transformations due to the abundance of starting materials, low cost, easy preparation, high thermal stability, facile reactivity and broad tolerance of functional groups on substrates [7,8]. Moreover, the use of cheaper earth-abundant metals such as copper in organic synthesis is appealing as a sustainable alternative [9–12].

In contrast to porous metal organic frameworks (MOFs), one-dimensional (1-D) CPs have scarcely been studied in catalysis. Whereas MOFs using rigid ligands retain their structural integrity during a catalytic reaction, CPs with flexible ligands allow the framework to respond reversibly to the presence of substrates [6,13,14]. This property could be of great interest in the development of new catalytic systems.

Over the last decade, flexible benzotriazole-based ligands have been used in the synthesis of CPs due to the coordinating ability of the benzotriazole moiety [15]. In these complexes, the metal center coordinates through the N3-nitrogen of the 1,2,3-triazole ring [1,2,13]. We have been interested in the synthesis and characterization of air-stable 1-D CPs through the self-assembly of copper(I) halides with *N*-donor bis(1*H*-benzotriazol-1-ylmethyl)arene ligands, as well as their uses in modified screen-printed electrodes for the voltammetric determination of dyes [1] and in transparent composite films for ultraviolet (UV) shielding [2]. Nevertheless, these CPs have not been studied in catalysis.

In this sense, the Cu(I)-catalyzed “click” azide-alkyne cycloaddition reaction gives easy access to 1,4-disubstituted 1,2,3-triazoles, which have applications in drug discovery and polymer synthesis [16,17]. In addition, this reaction tolerates a variety of functional groups, is insensitive to water and oxygen, and isolation of the products is simple [18,19]. These features led us to think that Cu(I) CPs might be added directly into the reaction mixture and be efficient catalysts for the “click” cycloaddition reaction, thus avoiding the use of excess ligand or additives. To the best of our knowledge, there are limited reports on the use of Cu(I) CPs for the azide-alkyne cycloaddition reaction [8].

According to our interest in exploring the role of CPs as catalysts in organic synthesis, we now report a new copper(I) benzotriazole-based

---

* Corresponding authors.
E-mail addresses: eperezh@uc.cl (E.G. Pérez), jj.hurtado@uniandes.edu.co (J.J. Hurtado).

https://doi.org/10.1016/j.ica.2019.119136
Received 15 July 2019; Received in revised form 5 September 2019; Accepted 6 September 2019

coordination polymer in one dimension (1-D) as an efficient catalyst for three-component azide-alkyne cycloadditions to obtain 1,4-disubstituted 1,2,3-triazoles from organic halides, sodium azide and terminal alkynes under mild reaction conditions ($T < 50\,^{\circ}C$, 5% mol catalyst, in air) and short reaction time ($t < 3$ h).

2. Experimental section

2.1. General

All reagents and solvents were purchased from commercial sources and used as received. All solvents used in this work were of analytical grade. The reactions were monitored by thin layer chromatography (TLC) on silica gel plates and observed under UV lamps (254 nm or 365 nm). The ligand 1,3-bis(1*H*-benzotriazol-1-ylmethyl)benzene (L) was prepared by a modified literature procedure [20–22], in one-step process at reflux, using commercially available reagents (*m*-xylylene dibromide and 1*H*-benzotriazole), and without using an organic base. Detailed synthesis and characterization are shown in the Supplementary Information.

NMR data were recorded on a Bruker Avance 400 spectrometer (400.13 MHz for ^{1}H; 100.61 MHz for ^{13}C). ^{1}H and ^{13}C NMR chemical shifts are reported in parts per million (ppm) relative to TMS, with the residual solvent peak used as an internal reference. High resolution mass spectra (HRMS) were obtained on an Agilent Technologies Q-TOF 6520 spectrometer *via* electrospray ionization (ESI) in the positive ion mode. Infrared spectra (FT-IR) were recorded on a Thermo Nicolet Nexus 470 ESP FT-IR spectrometer using KBr discs. Elemental analysis (C, H and N) was performed with a Thermo Scientific™ FLASH 2000 CHNS/O Analyzer. Thermogravimetric analysis (TGA) was performed on a NETZSCH STA 409 PC/PG instrument in a nitrogen atmosphere with a continuous flow of 100 mL min^{-1} and a heating rate of 10 °C min^{-1}, from 30 to 700 °C. Melting points were determined in open capillary tubes on a Mel-Temp® Electrothermal melting point apparatus and are uncorrected.

The electronic absorption spectra were measured in DMSO solution with a Varian Cary 100 Conc (Agilent Technologies) spectrophotometer from 200 to 800 nm, and in a quartz cuvette having a path length of 1 cm. Solid state emission and excitation spectra of the Cu(I) CP (at $\lambda_{ex} = 342$ nm; $\lambda_{em} = 538$ nm) were recorded by using a CARY Eclipse (Agilent Technologies) fluorescence spectrophotometer with the solid sample holder accessory at room temperature (20 °C). Both the excitation and emission slit widths were 5 nm. During the luminescence measurements, a low voltage detector was used for the complex due to its strong solid-state emission.

2.2. Synthesis of the 1-D Cu(I) coordination polymer catena-poly[bis-μ-[1,3-bis(1H-benzotriazol-κN^3-1-ylmethyl)benzene]dicopper(I)-di-μ-iodo]

CuI (241 mg, 1.24 mmol) was added to a solution of 1,3-bis(1*H*-benzotriazol-1-ylmethyl)benzene (400 mg, 1.16 mmol) in acetonitrile (24 mL). The resulting solution was stirred for 1 h at room temperature, giving a yellow solid. The precipitate was isolated by vacuum filtration, washed with acetonitrile, and dried under vacuum. Yield: 510 mg (82%). mp 236–238 °C. IR (KBr, cm^{-1}): ν 3059 (w), 3029 (w), 2969 (w), 2932 (w), 1611 (w), 1591 (w), 1497 (w), 1454 (m), 1313 (m), 1270 (w), 1224 (s), 1162 (m), 1135 (w), 1114 (m), 1002 (w), 971 (w), 901 (w), 779 (s), 757 (s), 741 (s). ^{1}H NMR (400 MHz, DMSO-d_6): δ (ppm) 8.05 (d, $J = 7.6$ Hz, 2H), 7.73 (d, $J = 8.1$ Hz, 2H), 7.46 (t, $J = 7.4$ Hz, 2H), 7.41 – 7.34 (m, 3H), 7.31 (d, $J = 7.1$ Hz, 1H), 7.25 (d, $J = 7.1$ Hz, 2H), 5.94 (s, 4H). Anal. Calcd. for $C_{20}H_{16}N_6CuI$: C, 45.25; H, 3.04; N, 15.83. Found: C, 44.20; H, 3.27; N, 15.10. HRMS (ESI+) *m/z* 341.1524 $[L + H]^+$, 592.9076 $[Cu_2I(L)]^+$, 743.2182 $[Cu(L)_2]^+$, 933.0518 $[Cu_2I(L)_2]^+$, 1124.8863 $[Cu_3I_2(L)_2]^+$. UV–vis (DMSO) [λ_{max} (log ε), nm (M^{-1} cm^{-1})]: 263 (4.29), 283 (4.12).

Table 1
Crystal data and structure refinement for Cu(I) CP.

Empirical formula	$C_{20}H_{16}CuIN_6$
Formula weight	530.83
Temperature/K	293(2)
Crystal system	Monoclinic
Space group	$P2_1/n$ (no. 14)
a/Å	11.2216(11)
b/Å	11.4710(11)
c/Å	15.0558(16)
α/°	90
β/°	92.770(6)
γ/°	90
Volume/Å^3	1935.8(3)
Z	4
ρ_{calc} g/cm^3	1.821
μ/mm^{-1}	14.261
F(0 0 0)	1040.0
Crystal size/mm^3	0.36 × 0.152 × 0.102
Radiation	Cu Kα (λ = 1.54178)
2Θ range for data collection/°	9.61 to 131.3
Index ranges	$-13 \le h \le 13$, $-13 \le k \le 13$, $-17 \le l \le 17$
Reflections collected	42,946
Independent reflections	3322 [$R_{int} = 0.1041$, $R_{sigma} = 0.0511$]
Data/restraints/parameters	3322/0/254
Goodness-of-fit on F^2	1.062
Final R indexes [I > = 2σ (I)]	$R_1 = 0.0591$, $wR_2 = 0.1155$
Final R indexes [all data]	$R_1 = 0.0984$, $wR_2 = 0.1347$
Largest diff. peak/hole/e Å^{-3}	0.65/−1.43

2.3. X-ray crystallography

Single crystals of the Cu(I) CP for X-ray structural analysis were obtained after a few days by slow evaporation in acetonitrile solution. A suitable crystal was selected and mounted using a MiTeGen MicroMount. Intensity data were collected at room temperature on a Bruker D8 VENTURE diffractometer equipped with a bidimensional CMOS Photon100 detector, using graphite monochromated Cu-Kα radiation. The structure solution and refinement were carried out with OLEX2 [23]. The structure was solved by direct methods using the SHELXS software [24]. The complete structure was refined by the full matrix least-squares procedures on the reflection intensities (F^2) with the SHELXL software [25]. All non-hydrogens were refined with anisotropic displacement coefficients, and all hydrogen atoms were placed in idealized locations. Molecular graphics were generated using Mercury 3.3 [26]. Color codes for molecular graphics were orange (Cu), blue (N), grey I, white (H) and purple (I). Crystal data and details of data collection for the Cu(I) CP are reported in Table 1.

Powder X-ray diffraction data were collected at room temperature on a Rigaku Ultima III X-ray diffractometer with Cu-Kα radiation (λ = 1.54056 Å). The samples were scanned using a step size of 0.02° and a scan speed of 2 s per step (Fig. S8, see Supplementary Information).

2.4. Computational details

Relativistic density functional theory calculations [27] were carried out using the ADF code [28], incorporating scalar (SR) corrections *via* the one-component ZORA Hamiltonian [29]. We employed the triple-ξ Slater basis set, plus two polarization functions (STO-TZ2P) for valence electrons, within the generalized gradient approximation (GGA) according to the Perdew-Burke-Ernzerhof (PBE) exchange-correlation functional [30,31] because of its improved performance on long-range interactions and relatively low computational cost [32–36]. The frozen core approximation was applied to the [1s^2-3p^6] shells for Cu, [1s^2-4p^6] for I, and [1s^2] for C and N, leaving the remaining electrons to be treated variationally. Geometry optimizations were performed without any symmetry restraint, *via* the analytical energy gradient method implemented by Versluis and Ziegler [37]. An energy convergence criterion of 10^{-4} Hartree, gradient convergence criteria of 10^{-3} Hartree/Å and radial convergence criteria of 10^{-2} Å were employed for the evaluation of the relaxed structures. The PBE functional at the scalar relativistic level and the Davidson method were employed in the TD-DFT calculations [38–41] to calculate the optical properties.

2.5. Catalytic activity for three-component azide-alkyne cycloadditions

Catalyst Cu(I) CP (5% mol), organic bromide (1.0 mmol), NaN_3 (1.2 mmol), alkyne (1.2 mmol) and CH_3CN (2 mL) were placed in a screw cap vial. Then, the reaction mixture was stirred at 50 °C and was monitored by TLC on silica gel plates using petroleum ether – ethyl acetate (2:1). The yields were determined *in situ* by ^{1}H NMR using a known quantity of 1,3,5-trimethoxybenzene as internal standard. After completion of the reaction, the solvent was evaporated under reduced pressure and the 1,2,3-triazole products were purified using silica gel column chromatography. All the products were characterized by ^{1}H and ^{13}C NMR, and ESI-HRMS spectra (Figs. S18–S32, see Supplementary Information).

3. Results and discussion

3.1. Synthesis and characterization of 1-D Cu(I) coordination polymer

The Cu(I) CP was synthesized efficiently by the self-assembly reaction of stoichiometric amounts of Cu(I) iodide and 1,3-bis(1*H*-benzotriazol-1-ylmethyl)benzene (L). The synthesis was performed at room temperature in acetonitrile, in the presence of air, with a short reaction time (1 h) and using a simple combination of reagents (Fig. 1). The product was obtained as a yellow solid in good yield (82%) with a melting point of 236–238 °C; moreover, it was air and moisture stable and insoluble in water and common organic solvents (e.g. chloroform, dichloromethane, ethyl acetate, acetone and ethanol). Neither the ligand nor the Cu(I) CP syntheses require the use of a glove box or Schlenk techniques. Besides, the purification is straightforward and does not involve the use of chromatography. The CP was structurally characterized as a 1-D coordination polymer with formula $[Cu_2(\mu\text{-}I)_2(\mu\text{-}L)_2]_n$, by means of infrared and photoluminescence spectroscopy, elemental and thermogravimetric analyses, single-crystal and powder X-ray diffraction. Elemental and thermogravimetric analyses of the Cu(I) CP are consistent with a 1:1 (metal:ligand) stoichiometry.

The thermogravimetric analysis (TGA) curve of the Cu(I) CP under nitrogen from 30 to 700 °C showed high thermal stability. The compound was found to be stable up to 314 °C (Fig. 2). This decomposition temperature (T_{dec}) is defined as the temperature of 5% weight loss [42]. During the heating process, the TGA curve showed two stages of weight loss at 344 and 614 °C. Finally, the remaining weight at 700 °C (34.6%, Calcd. 35.8%) is consistent with residual Cu(I) iodide.

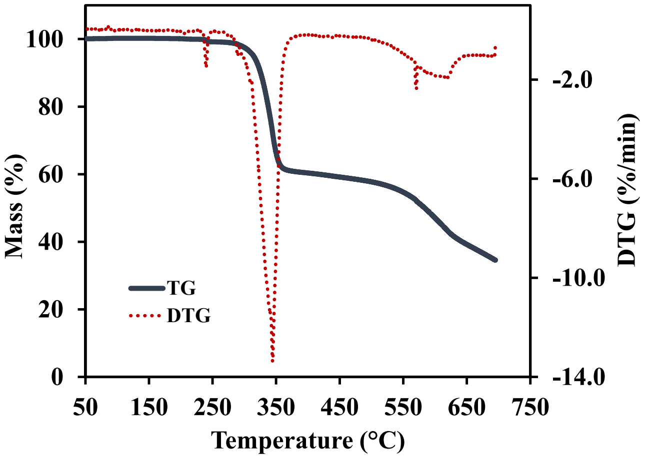

Fig. 2. Thermogravimetric analysis (TGA) and derivative thermogravimetry (DTG) of the Cu(I) CP in a nitrogen atmosphere.

The infrared (IR) spectrum of the Cu(I) CP showed the characteristic bands of the ligand (Figs. S5–S7). However, the band at 1313 cm^{-1}, assigned to the combination of the N=N stretching and ring breathing vibrations of benzotriazole, appears at a lower wavenumber compared to the free ligand (1342 cm^{-1}). The band at 1114 cm^{-1}, due to the N–N stretching vibration of the benzotriazole group, shifts towards higher wavenumbers when compared to the free ligand (1080 cm^{-1}) [43]. These results indicate that the benzotriazole moieties of the ligand are coordinated to the metal atom.

3.2. X-ray diffraction analysis

Suitable single crystals of the Cu(I) CP for X-ray diffraction (XRD) analysis were obtained after a few days by slow evaporation in acetonitrile solution. Single-crystal XRD analysis revealed that the complex consists of a 1-D coordination polymer with formula $[Cu_2(\mu\text{-}I)_2(\mu\text{-}L)_2]_n$ (Table 1, Figs. 1 and 3). The Cu(I) CP crystallizes in the monoclinic crystal system with space group $P2_1/n$ (14). The asymmetric unit contains one Cu(I) center, one iodine atom and one ligand L (Fig. 3a). In the molecular structure, the coordination geometry around the Cu atoms is distorted tetrahedral $Cu(N3_{bt})_2I_2$, considering coordination by two ligands through the N atoms in the 3-position of the benzotriazole rings and two iodine atoms. On the basis of the geometric parameters for coordination number CN = 4, τ_4 (0.92) and τ_4' (0.91) values, Cu atom adopts almost ideal tetrahedral geometry [44–46].The inorganic subunit in the compound is a $\{Cu_2(\mu\text{-}I)_2\}$ binuclear core with a planar rhomboid structure. The flexible organic ligand 1,3-bis(1*H*-benzotriazol-1-ylmethyl)benzene adopts a bidentate-bridging coordination mode, forming infinite linear chains and bridging the dimeric $\{Cu_2(\mu\text{-}$

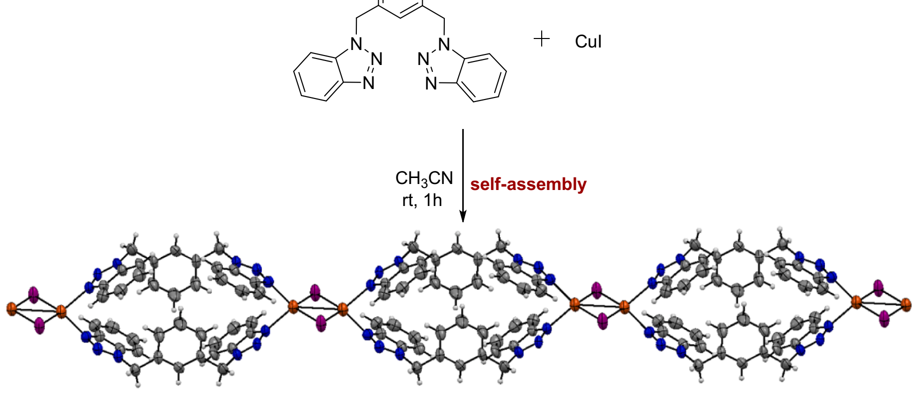

Fig. 1. Synthesis and molecular structure of the 1-D Cu(I) CP with displacement ellipsoids drawn at the 50% probability level. Copper, iodine, nitrogen and carbon atoms are shown in orange, purple, blue and grey, respectively. Hydrogen atoms are shown as spheres of arbitrary radius. (For interpretation of the references to color in this figure legend, the reader is referred to the web version of this article.)

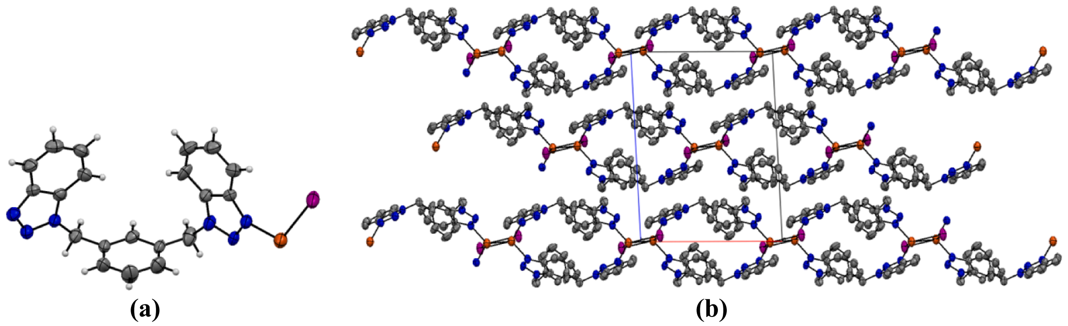

Fig. 3. (a) Asymmetric unit of the Cu(I) CP with displacement ellipsoids drawn at the 50% probability level. (b) Crystal packing of the 1-D Cu(I) CP. Hydrogen atoms are omitted for clarity.

I)$_2$} units as shown in Figs. 1 and 3b. This type of structure is similar to what we found in *catena*-poly[bis-μ-[2,6-bis(1*H*-benzotriazol-κN^3-1-ylmethyl)pyridine]dicopper(I)-di-μ-iodo], obtained from Cu(I) iodide and 2,6-bis(1*H*-benzotriazol-1-ylmethyl)pyridine [2]. The Cu···Cu distance in the {Cu$_2$(μ-I)$_2$} units is 2.829 Å, which is close to the sum of the van der Waals radii of copper(I) (2.8 Å), implying metal–metal bonding interactions. Literature data support Cu(I)···Cu(I) interactions with metal-to-metal distances in the range of 2.6 to 3.0 Å [47–51]. The multidentate and flexible ligand exhibits a bidentate-bridging coordination rather than a bidentate chelate coordination. Based on the crystal structure, the coordination polymer is formed under mild reaction conditions through a self-assembly process driven by metal-ligand coordination and is stabilized by metal-metal bonding interactions.

In order to confirm the identity and phase purity of the powder sample, a powder XRD pattern was analyzed using the Rietveld method based on the single crystal results (Figs. S8 and S9). The experimental powder XRD pattern for the Cu(I) CP matches its simulated pattern determined from the single-crystal XRD experiment, indicating the presence of mainly one crystalline phase in the bulk solid and showing that the single crystal structure is representative of the powder.

3.3. Photoluminescence studies

The solid-state excitation and emission spectra of the Cu(I) CP at room temperature showed a λ_{ex} = 342 nm and a strong green emission between 500 and 630 nm with a maximum at λ_{em} = 538 nm as shown in Fig. 4. In order to provide insights about the origin of the emission process, the optical properties of the Cu(I) CP have been studied theoretically. A molecular model involving three [Cu$_2$(μ-I)$_2$(μ-L)$_2$]$_n$ units (L = 1,3-bis(1*H*-benzotriazol-1-ylmethyl)benzene) was employed (Fig. S11) to evaluate the experimental excitation maximum and the corresponding emission by using time-dependent DFT calculations. The obtained optimized ground state structure agrees well with the characterization from X-ray diffraction, with Cu···Cu distances of 2.793 Å (Exp. 2.829 Å). The Cu—I distance is 2.673 Å (Exp. 2.606 Å), with a Cu—N length of 2.099 Å (Exp. 2.126 Å). Thus, the model is able to reproduce geometrical parameters of the extended CP structure.

For the Cu(I) CP, the calculated excitation maximum is located at 331 nm (Exp. 342 nm) involving a metal-to-ligand charge transfer (MLCT), from an orbital centered at {Cu$_2$(μ-I)$_2$} centered section to a ligand-localized orbital involving 1,3-bis(1*H*-benzotriazol-1-ylmethyl) benzene (Fig. 5). This spin-allowed transition leads to an excited singlet state (S$_n$*) with a ligand-based character, originated from the singlet ground state (S$_0$) as summarized in the given Jablonski diagram (Fig. 5). Interestingly, the $S_0 \rightarrow S_n*$ transition involves a charge transfer from the {Cu$_2$(μ-I)$_2$} core towards the benzotriazole moiety, in a metal-to-ligand charge transfer (MLCT) process. Next, a non-radiative intersystem crossing (ISC) gives the respective triplet excited state (T$_n$*), followed by a non-radiative decay towards the lowest energy triplet excited state (T$_1$*), which in turn leads to the phosphorescence calculated at 543 nm (Exp. 538 nm), in agreement to the Kasha's rule [52]. The lowest triplet excited state (T$_1$*) is centered in the benzyl group attached to the benzotriazole derivative. Overall, the computational results show that the entire excitation-emission process can be described as a {Cu$_2$(μ-I)$_2$} core → ligand centered transition, and a radiative decay from a benzotriazole-functional group localized orbital to recover the ground-state (S$_0$). Moreover, the experimental excitation and emission maxima wavelengths of the Cu(I) CP are slightly different from those that we observed in *catena*-poly[bis-μ-[2,6-bis(1*H*-benzotriazol-κN^3-1-ylmethyl) pyridine]dicopper(I)-di-μ-iodo] (λ_{ex} = 323 nm;

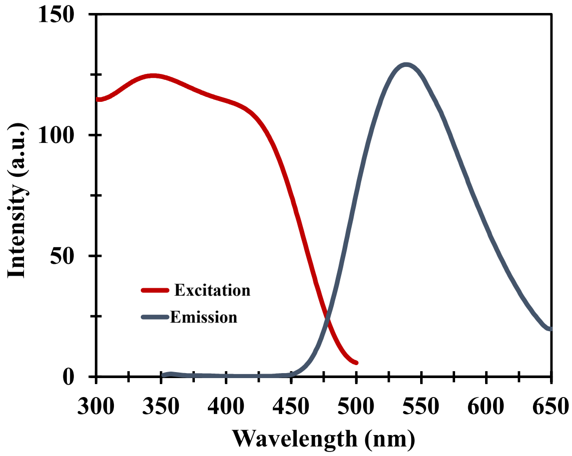

Fig. 4. Solid state excitation and emission spectra of the Cu(I) CP (λ_{ex} = 342 nm; λ_{em} = 538 nm) at room temperature.

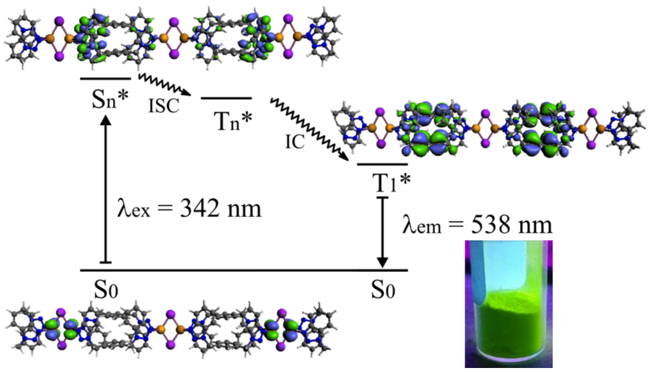

Fig. 5. Jablonski diagram showing the proposed radiative pathways for the 1-D Cu(I) CP. The CP exhibited strong green photoluminescence at room temperature in the solid state (λ_{em} = 538 nm). Fluorescence response in the picture was excited at 365 nm using a UV lamp. (For interpretation of the references to color in this figure legend, the reader is referred to the web version of this article.)

$\lambda_{em} = 532$ nm) [2]. Nevertheless, these types of coordination polymers could be considered as useful structural templates to tailor the emissive wavelength according to the selected benzotriazole functionalization.

The behavior of the Cu(I) CP was investigated in solution by ^1H NMR, UV–vis spectroscopy and high-resolution mass spectrometry (HRMS) using electrospray ionization (ESI). The compound was insoluble in common organic solvents and water, but a small amount could be dissolved using strongly coordinating solvents such as DMSO and acetonitrile. In solution, the complex loses its luminescence. The ^1H NMR spectrum of the Cu(I) CP in DMSO-d_6 showed no changes in the chemical shifts (δ) of the ligand (Figs. S1, S3 and S4). The UV–visible absorption spectrum of the free ligand in DMSO showed the absorption bands of π-π^* transitions at 264 and 284 nm (Fig. S12). The UV–vis spectrum of the Cu(I) CP in DMSO showed that the absorption bands of the ligand were not significantly affected by the metal atom (Fig. S13). The HRMS (ESI+) spectrum of the Cu(I) CP in acetonitrile exhibited the ion peaks (m/z) of $[Cu_3I_2(L)_2]^+$, $[Cu_2I(L)_2]^+$, $[Cu(L)_2]^+$, $[Cu_2I(L)]^+$ and $[L + H]^+$ (Figs. S14–S17). The isotopic peak patterns support the presence of copper (Fig. S16). These results suggested the loss of luminescence as a result of the decomplexation of the coordination polymer in polar aprotic solvents with high dielectric constant.

3.4. *Catalytic activity for three-component azide-alkyne cycloadditions*

It was found that the Cu(I) CP serves as an efficient supramolecular catalyst for three-component azide-alkyne cycloadditions to obtain 1,4-disubstituted 1,2,3-triazoles from organic halides, sodium azide and terminal alkynes under mild reaction conditions ($T < 50$ °C, 5% mol catalyst, in air) and short reaction time ($t < 3$ h). Moreover, no additional base or reducing agent is required, and the isolation and purification of organic azides are avoided in this one-pot synthesis.

Screening of reaction conditions revealed that CH_3CN was the most suitable solvent (Table 2, entry 12), and the reaction did not take place in the absence of Cu(I) species (Table 2, entry 8). Furthermore, the isolated Cu(I) CP catalyst (Table 2, entry 12) showed higher catalytic activity than the Cu(I) CP formed *in situ* during the catalysis under the same reaction conditions (Table 2, entry 13). Results are summarized in Tables 2 and 3. The 1,4-disubstituted 1,2,3-triazoles were obtained in good to excellent yields (62–95%) and the spectral data were in agreement with those described in the literature [18,53,54]. The compound 3-(1-(3-chlorobenzyl)-1*H*-1,2,3-triazol-4-yl)propan-1-ol is new (Figs. S18–S32). This Cu(I) CP-catalyzed synthesis was effective for alkynes with various functional groups (arene, alcohol and alkane) (Table 3).

Table 2
Optimization of the reaction conditions.[a]

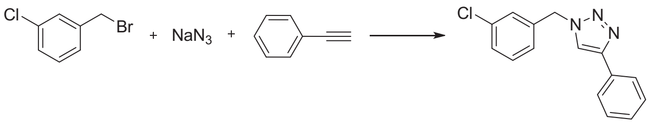

Entry	Catalyst	% mol	T (°C)	Time (h)	Solvent	Yield (%)
1	Cu(I) CP	2	r.t.	2	CH_3CN	trace
2	CuI	2	r.t.	2	CH_3CN	trace
3	Cu(I) CP	2	80	2	CH_3CN	29
4	Cu(I) CP	5	80	2	CH_3CN	55
5	Cu(I) CP	10	80	2	CH_3CN	83
6	Cu(I) CP	5	80	3	CH_3CN	94[b]
7	CuI	5	80	3	CH_3CN	84[b]
8	–	–	80	3	CH_3CN	n.r.
9	Cu(I) CP	5	80	3	EtOH	37
10	Cu(I) CP	5	80	3	DCE	n.r.
11	Cu(I) CP	5	80	3	CH_3CN-H_2O (1:1)	81
12	Cu(I) CP	5	50	3	CH_3CN	95[b]
13	Cu(I) CP[c]	5	50	3	CH_3CN	85
14	CuI	5	50	3	CH_3CN	74[b]

[a] ^1H NMR yields using 1,3,5-trimethoxybenzene as internal standard.
[b] Isolated by column chromatography.
[c] Cu(I) CP formed *in situ*.

Table 3
Cu(I) CP-catalyzed synthesis of 1,4-disubstituted 1,2,3-triazoles.[a]

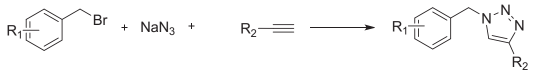

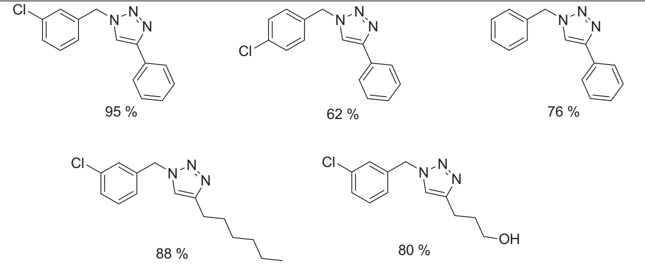

[a] Optimal conditions found in Table 2 (entry 12).

We hypothesize that the 1-D Cu(I) CP can act as a reservoir of active Cu(I) catalyst species in solution as is shown in Fig. S17 [16]. The Cu(I) CP catalyst showed higher catalytic activity than the salt copper(I) iodide under the same reaction conditions (Table 2, entry 14), which suggests that the coordination with the *N*-donor ligand decreases the Lewis acidity of the metal center, facilitating the reaction. According with Zhu and co-workers, the triple bond of a terminal alkyne could be a π acceptor from an electron-rich metal center (π-backbonding with copper(I)) and assist the formation of the copper/alkyne/azide ternary complex predisposed for cycloaddition [55]. Furthermore, the higher catalytic activity might be attributed to the synergistic effect between the two metal centers in the binuclear $\{Cu_2(\mu\text{-}I)_2\}$ core (Fig. 1), as proposed recently by Guo, Ye and co-workers for binuclear complexes [8,56]. Future work within our group will focus on the mechanism of this 1-D Cu(I) CP-catalyzed click reaction.

4. Conclusions

In conclusion, we have reported the synthesis and structural characterization of a new one-dimensional (1-D) coordination polymer with the formula $[Cu_2(\mu\text{-}I)_2(\mu\text{-}L)_2]_n$. This compound was easily obtained through a self-assembly process of copper(I) iodide with the ligand 1,3-bis(1*H*-benzotriazol-1-ylmethyl)benzene (L) and was isolated in good yield (82%) as an air- and moisture-stable solid. The flexible organic ligand adopted a bidentate-bridging coordination mode, forming infinite linear chains and bridging the binuclear $\{Cu_2(\mu\text{-}I)_2\}$ core. The CP exhibited high thermal stability and strong green photoluminescence at room temperature. The catalytic activity of the CP was studied in click chemistry, which revealed good performance in three-component azide-alkyne cycloadditions to obtain 1,4-disubstituted 1,2,3-triazoles in good to excellent yields from organic halides, sodium azide and terminal alkynes. Finally, the facile synthesis of these types of 1-D coordination polymers and the possibility of chemical modification of the organic ligand for tuning make Cu(I) CPs promising candidates for catalysis.

Declaration of Competing Interest

The authors declare that they have no known competing financial interests or personal relationships that could have appeared to influence the work reported in this paper.

Acknowledgements

The authors thank the School of Science of the Universidad de los Andes for financial support (project no. INV-2017-65-1683). N. Nuñez-Dallos is also grateful to COLCIENCIAS for his doctoral scholarship (Conv. 617) and to Universidad de Boyacá. E.G. Pérez is grateful for financial support from the Fondo Nacional para el Desarrollo Científico y Tecnológico, Chile (FONDECYT grant 1171391).

Appendix A. Supplementary data

Supplementary information available: experimental details and characterization data of compounds. CCDC 1545790 contains the supplementary crystallographic data for this paper. These data can be obtained free of charge from the Cambridge Crystallographic Data Center via www.ccdc.cam.as.uk/data_request/cif.

Supplementary data to this article can be found online at https://doi.org/10.1016/j.ica.2019.119136.

References

[1] N. Nuñez-Dallos, M.A. Macías, Olimpo García-Beltrán, J.A. Calderón, E. Nagles, J. Hurtado, J. Electroanal. Chem. 822 (2018) 95–104.
[2] N. Nuñez-Dallos, N. Lopez-Barbosa, A. Muñoz-Castro, D. Mac-Leod Carey, A. De Nisi, M. Monari, J.F. Osma, J. Hurtado, J. Coord. Chem. 70 (2017) 3363–3378.
[3] R.-Y. Wang, X. Zhang, J.-H. Yu, J.-Q. Xu, Photochem. Photobiol. Sci. 18 (2019) 477–486.
[4] T. Wen, D.-X. Zhang, J. Zhang, Inorg. Chem. 52 (2013) 12–14.
[5] Y.-L. Hou, R.W.-Y. Sun, X.-P. Zhou, J.-H. Wang, D. Li, Chem. Commun. 50 (2014) 2295–2297.
[6] E. Loukopoulos, G.E. Kostakis, J. Coord. Chem. 71 (2018) 371–410.
[7] X. Wang, M. Liu, Y. Wang, H. Fan, J. Wu, C. Huang, H. Hou, Inorg. Chem. 56 (2017) 13329–13336.
[8] X. Guo, C. Huang, H. Yang, Z. Shao, K. Gao, N. Qin, G. Li, J. Wu, H. Hou, Dalton. Trans. 47 (2018) 16895–16901.
[9] J. Saavedra-Olavarría, M. Madrid-Rojas, I. Almodovar, P. Hermosilla-Ibáñez, E.G. Pérez, RSC Adv. 8 (2018) 27919–27923.
[10] G.C. Arteaga, J. Saavedra-Olavarría, S. Almendras, P. Hermosilla-Ibáñez, I. Almodovar, E.G. Pérez, Tetrahedron Lett. 59 (2018) 1091–1093.
[11] C. Herrera-Leyton, M. Madrid-Rojas, J.J. López, Á. Cañete, P. Hermosilla-Ibáñez, E.G. Pérez, ChemCatChem 8 (2016) 2015–2018.
[12] J. Saavedra-Olavarría, G.C. Arteaga, J.J. López, E.G. Pérez, Chem. Commun. 51 (2015) 3379–3382.
[13] E. Loukopoulos, N.F. Chilton, A. Abdul-Sada, G.E. Kostakis, Cryst. Growth Des. 17 (2017) 2718–2729.
[14] M. Kallitsakis, E. Loukopoulos, A. Abdul-Sada, G.J. Tizzard, S.J. Coles, G.E. Kostakis, I.N. Lykakis, Adv. Synth. Catal. 359 (2017) 138–145.
[15] E. Loukopoulos, G.E. Kostakis, Coord. Chem. Rev. 395 (2019) 193–229.
[16] L.D. Pachón, J.H. van Maarseveen, G. Rothenberg, Adv. Synth. Catal. 347 (2005) 811–815.
[17] E. Loukopoulos, A. Abdul-Sada, G. Csire, C. Kállay, A. Brookfield, G.J. Tizzard, S.J. Coles, I.N. Lykakis, G.E. Kostakis, Dalton Trans. 47 (2018) 10491–10508.
[18] M.K. Barman, A.K. Sinha, S. Nembenna, Green Chem. 18 (2016) 2534–2541.
[19] H.G. Hosseini, E. Doustkhah, M.V. Kirillova, S. Rostamnia, G. Mahmoudi, A.M. Kirillov, Appl. Catal. A Gen. 548 (2017) 96–102.
[20] M.A. Macías, N. Nuñez-Dallos, J. Hurtado, L. Suescun, Acta Cryst. E 72 (2016) 815–818.
[21] P. Rajakumar, V. Murali, Tetrahedron 56 (2000) 7995–7999.
[22] B.J. O'Keefe, P.J. Steel, Inorg. Chem. Commun. 3 (2000) 473–475.
[23] O.V. Dolomanov, L.J. Bourhis, R.J. Gildea, J.A.K. Howard, H. Puschmann, J. Appl. Cryst. 42 (2009) 339–341.
[24] G.M. Sheldrick, IUCr, *Acta Cryst. A* 64 (2008) 112–122.
[25] G.M. Sheldrick, Acta Cryst. C 71 (2015) 3–8.
[26] C.F. Macrae, I.J. Bruno, J.A. Chisholm, P.R. Edgington, P. McCabe, E. Pidcock, L. Rodriguez-Monge, R. Taylor, J. van de Streek, P.A. Wood, J. Appl. Cryst. 41 (2008) 466–470.
[27] K.G. Dyall, K. Fægri, Introduction to Relativistic Quantum Chemistry, Oxford University Press, New York, 2007.
[28] Amsterdam Density Funct. code, Release 2013, SCM, Theor. Chem. Vrije Univ. Amsterdam, Netherlands, 2013.
[29] E. van Lenthe, E.J. Baerends, J.G. Snijders, J. Chem. Phys. 101 (1994) 9783–9792.
[30] J.P. Perdew, K. Burke, Y. Wang, Phys. Rev. B 54 (1996) 16533–16539.
[31] J.P. Perdew, K. Burke, M. Ernzerhof, Phys. Rev. Lett. 78 (1997) 1396–1396.
[32] O. Lopez-Acevedo, J. Akola, R.L. Whetten, H. Grönbeck, H. Häkkinen, J. Phys. Chem. C 113 (2009) 5035–5038.
[33] J. Akola, M. Walter, R.L. Whetten, H. Häkkinen, H. Grönbeck, J. Am. Chem. Soc. 130 (2008) 3756–3757.
[34] D. Jiang, Nanoscale 5 (2013) 7149.
[35] J. Akola, K.A. Kacprzak, O. Lopez-Acevedo, M. Walter, H. Grönbeck, H. Häkkinen, J. Phys. Chem. C 114 (2010) 15986–15994.
[36] D. Jiang, M. Kühn, Q. Tang, F. Weigend, J. Phys. Chem. Lett. 5 (2014) 3286–3289.
[37] L. Versluis, T. Ziegler, J. Chem. Phys. 88 (1988) 322–328.
[38] A. Rosa, E.J. Baerends, S.J.A. van Gisbergen, E. van Lenthe, J.A. Groeneveld, J.G. Snijders, J. Am. Chem. Soc. 121 (1999) 10356–10365.
[39] S.J.A. van Gisbergen, J.G. Snijders, E.J. Baerends, Comput. Phys. Commun. 118 (1999) 119–138.
[40] F. Wang, T. Ziegler, E. van Lenthe, S. van Gisbergen, E.J. Baerends, J. Chem. Phys. 122 (2005) 204103.
[41] F. Wang, T. Ziegler, J. Chem. Phys. 123 (2005) 194102.
[42] F. Wu, J. Li, H. Tong, Z. Li, C. Adachi, A. Langlois, P.D. Harvey, L. Liu, W.-Y. Wong, W.-K. Wong, X. Zhu, J. Mater. Chem. C 3 (2015) 138–146.
[43] S.G. Aziz, S.A. Elroby, A. Alyoubi, O.I. Osman, R. Hilal, J. Mol. Model. 20 (2014) 2078.
[44] L. Yang, D.R. Powell, R.P. Houser, Dalton Trans. (2007) 955–964.
[45] A. Okuniewski, D. Rosiak, J. Chojnacki, B. Becker, Polyhedron 90 (2015) 47–57.
[46] B. Cordero, V. Gómez, A.E. Platero-Prats, M. Revés, J. Echeverría, E. Cremades, F. Barragán, S. Alvarez, Dalton Trans. (2008) 2832.
[47] A. Gallego, C. Hermosa, O. Castillo, I. Berlanga, C.J. Gómez-García, E. Mateo-Martí, J.I. Martínez, F. Flores, C. Gómez-Navarro, J. Gómez-Herrero, S. Delgado, F. Zamora, Adv. Mater. 25 (2013) 2141–2146.
[48] H. Araki, K. Tsuge, Y. Sasaki, S. Ishizaka, N. Kitamura, Inorg. Chem. 44 (2005) 9667–9675.
[49] M.-C. Hu, Y. Wang, Q.-G. Zhai, S.-N. Li, Y.-C. Jiang, Y. Zhang, Inorg. Chem. 48 (2009) 1449–1468.
[50] J. Pan, C.-P. Liu, F.-L. Jiang, M.-Y. Wu, L. Chen, J.-J. Qian, K.-Z. Su, X.-Y. Wan, M.-C. Hong, CrystEngComm 17 (2015) 1541–1548.
[51] S.-Q. Bai, L. Jiang, B. Sun, D.J. Young, T.S.A. Hor, CrystEngComm 17 (2015) 3305–3311.
[52] M. Kasha, Discuss. Faraday Soc. 9 (1950) 14–19.
[53] S.R. Kale, S.S. Kahandal, M.B. Gawande, R.V. Jayaram, RSC Adv. 3 (2013) 8184.
[54] C. Menendez, A. Chollet, F. Rodriguez, C. Inard, M.R. Pasca, C. Lherbet, M. Baltas, Eur. J. Med. Chem. 52 (2012) 275–283.
[55] L. Zhu, C.J. Brassard, X. Zhang, P.M. Guha, R.J. Clark, Chem. Rec. 16 (2016) 1501–1517.
[56] W. Ye, X. Xiao, L. Wang, S. Hou, C. Hu, Organometallics 36 (2017) 2116–2125.